

# In-medium modification and decay asymmetry of $\omega$ mesons in cold nuclear matter

A.I. Titov<sup>a,b</sup> and B. Kämpfer<sup>a,c</sup>

<sup>a</sup>*Forschungszentrum Dresden-Rossendorf, 01314 Dresden, Germany*

<sup>b</sup>*Bogoliubov Laboratory of Theoretical Physics, JINR, Dubna 141980, Russia*

<sup>c</sup>*Institut für Theoretische Physik, TU Dresden, 01062 Dresden, Germany*

## Abstract

We discuss an asymmetry of the decay  $\omega \rightarrow e^+e^-$  in nuclear matter with respect to the electron and positron energies. This asymmetry is sensitive to the properties of the  $\omega$  meson self-energy and, in particular, it has a non-trivial dependence on the  $\omega$  energy and momentum. Therefore, this asymmetry may serve as a powerful tool in studying the properties of the  $\omega$  meson in the nuclear medium.

PACS numbers: 13.88.+e, 13.60.Le, 14.20.Gk, 25.20.Lj

Keywords:  $\omega$  meson in nuclear matter, decay asymmetry

## I. INTRODUCTION

The study of in-medium properties of light vector mesons is a topic of great importance for hadron and heavy-ion physics. Besides the hope to get information on the mechanism of how hadrons acquire their masses, the in-medium modifications are related to the chiral symmetry restoration and changes of the QCD vacuum structure [1]. Otherwise, vector mesons decaying into  $e^+e^-$  pairs can provide unique information about the evolution of nuclear matter in relativistic heavy-ion collisions as a penetrating probe, not suffering final state interactions [1]. Vector meson properties may not only be changed in compressed and heated strongly interacting matter but also at normal baryon density and zero temperature.

We will concentrate on the properties of the  $\omega$  meson being a hadron with a small decay width thus providing a unique probe for the expected in-medium modifications. The interaction of the  $\omega$  meson with surrounding nucleons, nucleon resonances, and exchange-meson currents are thought to lead to modifications of  $\omega$  meson propagating in a nucleus. First experimental results of such modifications have been reported in Refs. [2, 3]. Much theoretical work has been devoted for an evaluation of the  $\omega$  meson self-energy as key quantity for the prediction of spectral properties. The calculations point to an increase of  $\omega$  width reflecting the opening of new inelastic channels. But the predictions for the  $\omega$  spectral function, often condensed into one quantity – the mass, are wildly differing in different models as the scale (and even the sign) of the mass modification depends on the assumed dynamics of the  $\omega$  interaction with the ambient nuclear medium. For instance, the models of Refs. [4–8] predict a shift of the peak position of the  $\omega$  spectral function to lower energy, whereas results of some other approaches [9–13, 15] show an upward shift.

As a rule, the available estimates of the self-energy are made within the low-energy theorem [16], where the in-medium part of the self-energy is expressed through the  $\omega N$  forward scattering amplitude. In fact, in different models, different components and channels of the  $\omega N$  amplitude are assumed to be important. For simplicity, in the following discussion we limit our considerations to the contribution of such baryon resonances which seem to be dominant not only in the Compton  $\omega N$  scattering amplitude but also in  $\omega$  production in photon-nucleon [17–21], meson-nucleon [22, 23] and proton-proton ( $pp$ ) reactions [24, 25] near the threshold of  $\omega$ .

In different models, different resonances become dominant. Thus, for example, for  $\omega$  me-

son production in  $pp$  reactions, Ref. [24] argues for a dominance of  $P_{11}(1710)$  and  $D_{13}(1700)$  resonances, while in Ref. [25] the dominant contribution comes from  $S_{11}(1535)$  and  $S_{11}(1650)$ . A similar situation is met in  $\omega$  meson photo-production: In Refs. [11, 23], a strong contribution to the  $\omega N$  channel comes from  $S_{11}(1535)$ ,  $S_{11}(1650)$ , and  $D_{13}(1520)$  resonances, while in Refs. [18, 20, 21] a significant contribution stems from spin-5/2 resonances. In Refs. [18, 20, 21], it is  $F_{15}(1680)$ , while the analysis of Ref. [19] supports a  $P_{11}(1710)$  resonance. These ambiguities are extended to the  $\omega$  meson self-energy and the related current-current correlation function.

In order to reduce the mentioned ambiguities, it would be nice to have, together with the position and width of the resonance in the current-current correlation function, additional observables being sensitive to the dynamics of the  $\omega N$  interaction. One possible candidate is the asymmetry of the di-electron angular or energy distribution related to the difference of the transverse and longitudinal parts of the  $\omega$  meson self-energy in a nuclear medium. This difference disappears for the  $\omega$  meson at rest (relative to the nuclear medium) and becomes finite for a finite  $\omega$  meson momentum  $\mathbf{q}$ . High-spin resonances can be excited only by the orbital interaction, and therefore, they do not contribute at  $\mathbf{q} = 0$ . When  $|\mathbf{q}|$  increases, they become important. The dependence of the transverse and longitudinal parts of the partial amplitudes on the  $\omega$  meson mass and momentum and, therefore, the asymmetry between transverse and longitudinal parts of the current-current correlation function may be used as a tool for fixing the mechanism of the relevant  $\omega N$  interaction. This has a practical aspect since most of experiments studying the in-medium  $\omega$  meson properties are dealing with non-zero  $\omega$  meson momenta.

The aim of our paper is the discussion of an example of such an asymmetry. We introduce the asymmetry between the transverse and longitudinal parts of the current-current correlation function and, as mere illustration, we apply it to a simple resonance model of the  $\omega N$  scattering. In fact, it is the same model which was used previously for  $\omega$  photo-production in Ref. [18].

Our paper is organized as follows. In Sec. II we introduce the asymmetry of the  $\omega \rightarrow e^+e^-$  decay. In Sec. III we present a model for current-current correlation function in nuclear medium, where the  $\omega N$  interaction is described by a resonance model. Numerical results and a discussion are given in Sec. IV. The summary can be found in Sec. V. The appendices contain a brief recollection of the  $\omega$  self-energy in vacuum and the effective Lagrangians and

coupling strengths employed here.

## II. ASYMMETRY OF $\omega \rightarrow e^+e^-$ DECAY

We assume that the  $\omega$  meson is produced in the inclusive reaction  $a + A \rightarrow \omega + X$ , where the projectile  $a$  may be a photon or hadron. Then, the  $\omega$  meson propagates in the nuclear medium of the target nucleus  $A$  and afterwards decays into a electron-positron pair. Our starting point is the well known relation between the differential di-electron production rate  $dR$  and the current-current correlator (CCC)  $\Pi_{\mu\nu}$  [26, 27]

$$dR = \frac{e^2}{q^4} \mathcal{L}^{\mu\nu} \text{Im}\Pi_{\mu\nu} \frac{d\mathbf{p}_+}{2E_+} \frac{d\mathbf{p}_-}{2E_-}. \quad (1)$$

In the following, the four-momenta of  $\omega$  meson, outgoing electron and positron are denoted as  $q = (\omega, \mathbf{q})$  and  $p_{\pm} = (E_{\pm}, \mathbf{p}_{\pm})$ , respectively. The masses of the virtual  $\omega$  meson and electron/positron are defined as  $M = \sqrt{q^2}$  and  $M_e$ , respectively. The quantization axis ( $\mathbf{z}$ ) is chosen along direction of the  $\omega$  meson velocity. The lepton tensor reads

$$\frac{1}{4} \mathcal{L}_{\mu\nu} = p_{+\mu} p_{-\nu} + p_{-\mu} p_{+\nu} - g_{\mu\nu} (p_- \cdot p_+ + M_e^2). \quad (2)$$

The imaginary part of the CCC can be decomposed in longitudinal and transverse parts as

$$-\text{Im}\Pi_{\mu\nu} = W^L P_{\mu\nu}^L + W^T P_{\mu\nu}^T, \quad (3)$$

where  $P_{\mu\nu}^L$  and  $P_{\mu\nu}^T$  are the standard longitudinal and transverse polarization tensors,

$$\begin{aligned} P_{\mu\nu}^L &= \left( u_{\mu} - q_{\mu} \frac{u \cdot q}{q^2} \right) \left( u_{\nu} - q_{\nu} \frac{u \cdot q}{q^2} \right) \frac{q^2}{q^2 u^2 - (u \cdot q)^2}, \\ P_{\mu\nu}^T &= P_{\mu\nu}^0 - P_{\mu\nu}^L, \quad P_{\mu\nu}^0 = \left( g_{\mu\nu} - \frac{q_{\mu} q_{\nu}}{q^2} \right), \end{aligned} \quad (4)$$

and  $u = (1, \mathbf{0})$  is the four-velocity of the medium wherein the  $\omega$  meson propagates. Then, one gets with  $q = p_+ + p_-$  the following relations

$$\begin{aligned} \mathcal{L}^{\mu\nu} P_{\mu\nu}^L &= -2q^2 \left( 1 - \frac{(E_+ - E_-)^2}{\mathbf{q}^2} \right), \\ \mathcal{L}^{\mu\nu} P_{\mu\nu}^T &= -2q^2 \left( 1 + \frac{(E_+ - E_-)^2}{\mathbf{q}^2} + \epsilon \right) \end{aligned} \quad (5)$$

with  $\epsilon = 4M_e^2/M^2$ . We are interested in di-electron production with invariant mass  $M \gg 2M_e$  and, therefore, all terms proportional to  $\epsilon$  can be omitted.

For later purposes we introduce a useful variable in the medium's rest frame

$$\xi = \frac{E_+ - E_-}{|\mathbf{q}|} . \quad (6)$$

The electron energy  $E_e$  and the variable  $\xi$  are defined in the regions

$$\omega - |\mathbf{q}| \leq 2E_e \leq \omega + |\mathbf{q}|, \quad -1 \leq \xi \leq 1. \quad (7)$$

Integrating Eq. (1) over the azimuthal angle of the decay plane, one can express the differential di-electron production rate in terms of the variables  $\xi$  and  $q$

$$\frac{d^5 R(M, \mathbf{q})}{d^4 q d\xi} = \frac{\pi e^2}{2q^2} (W^L(1 - \xi^2) + W^T(1 + \xi^2)) . \quad (8)$$

Integration of this equation over  $\xi$  leads to the famous rate

$$\frac{d^4 R(M, \mathbf{q})}{d^4 q} = \frac{2\pi e^2}{3q^2} (W^L + 2W^T) . \quad (9)$$

Equation (8) allows us to define the asymmetry

$$\mathcal{A}(\xi) = \frac{d^4 R(\xi) - d^4 R(0)}{d^4 R(0)} = \xi^2 \mathcal{A}^{TL} \quad (10)$$

with

$$\mathcal{A}^{TL} = \frac{W^T - W^L}{W^T + W^L} . \quad (11)$$

One can see that the asymmetry with respect to the difference of the electron and positron energies is directly related to the asymmetry between longitudinal and transverse parts of the CCC. The asymmetry can be expressed as a function of the angle  $\alpha$  between the two vectors  $\mathbf{q} = \mathbf{p}_+ + \mathbf{p}_-$  and  $\mathbf{t} = \mathbf{p}_+ - \mathbf{p}_-$ ,

$$\xi^2 \simeq \frac{\cos^2 \alpha}{\cos^2 \alpha + \gamma^2 \sin^2 \alpha} , \quad (12)$$

where  $\gamma = \omega/M$  is the Lorentz factor of the  $\omega$  meson. The angle  $\alpha$  is equal to  $\pi/2$  for  $\xi = 0$  (i.e.  $E_+ = E_-$ ), and  $\alpha = 0$  for  $\xi = 1$  (i.e.  $E_{\pm} = E_{\min}^{\max}$ ), as depicted in Fig. 1. Therefore, the asymmetry  $\mathcal{A}(\xi)$  may be considered as a measure of the anisotropy of the  $\omega \rightarrow e^+e^-$  decay [27–29]. For a slowly moving  $\omega$  meson with  $\gamma \simeq 1$ , we have  $\xi^2 \simeq \cos^2 \alpha$ , and the angle  $\alpha$  is close to the polar angle of the direction of the electron momentum with respect to the direction of the  $\omega$  meson momentum.

If the  $\omega$  meson is in rest ( $\mathbf{q} = 0$ ), with respect to the medium's rest frame, then  $W^T = W^L$  and the asymmetry  $\mathcal{A}^{TL}$  is equal to zero. At finite  $\mathbf{q}$ , the asymmetry becomes non-zero and depends on the properties of the  $\omega$  meson self-energy [26–29]. In the general case,  $\mathcal{A}^{TL}$  is a non-trivial function of  $M$  and  $\mathbf{q}$  as shown below.

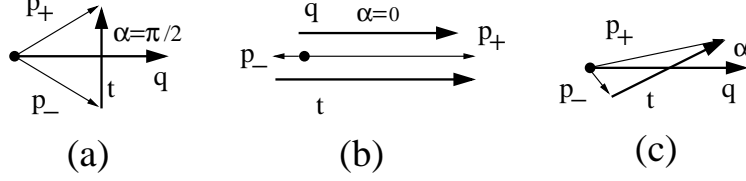


FIG. 1: Geometry of the  $\omega \rightarrow e^+e^-$  decay. (a) and (b) correspond to cases where  $\alpha = \pi/2$  (i.e.  $\xi = 0$ ) and  $\alpha = 0$  (i.e.  $\xi = 1$ ), respectively, while (c) depicts an intermediate case  $0 < \alpha < \pi/2$  (i.e.  $0 < |\xi| \leq 1$ ).

### III. MODEL FOR CURRENT-CURRENT CORRELATION FUNCTION IN BARYON MEDIUM

Usually, the CCC is defined within the vector dominance model based on the current-field identity [30] for the electromagnetic current  $\mathcal{J}_\mu$

$$\mathcal{J}_\mu = - \sum_V \frac{eM_V^2}{2\gamma_V} V_\mu, \quad (13)$$

where  $M_V$  ( $V = \rho, \omega, \phi \dots$ ) is the vector meson mass and  $2\gamma_V \equiv g_V$  is a dimensionless constant, which can be determined from the partial  $V \rightarrow e^+e^-$  decay widths as  $\gamma_\rho/\gamma_\omega/\gamma_\phi \simeq 2.5/8.5/6.7$ . We focus here on the  $\omega$  contribution. An explicit expression for the CCC can be derived using diagrammatic techniques (see, for example, Ref. [5]). The imaginary part of  $\Pi$  is related to the  $\omega$  meson self-energy as

$$\left[ \frac{e^2 M_{\omega 0}^4}{g_\omega^2} \right]^{-1} \text{Im} \Pi^{ccL(T)} \equiv -W^{L(T)} = \frac{\text{Im} \Pi_\omega^{L(T)}}{|q^2 - M_{\omega 0}^2 - \Pi_\omega^{L(T)}|^2}, \quad (14)$$

where  $M_{\omega 0}$  is a "bare"  $\omega$  meson mass and  $\Pi_\omega^{L(T)}$  represents the longitudinal (transverse) part of the full  $\omega$  meson self-energy. At low baryon density, following the low-density theorem [16], the full  $\omega$  meson self-energy is expressed as a sum of its vacuum part and the contribution from the Compton  $\omega N$  scattering [5, 15]

$$\Pi_{\omega\mu\nu} = \Pi_{\omega\mu\nu}^{\text{vac}} + \tilde{\rho} T_{\mu\nu}^{\omega N}, \quad (15)$$

where  $\tilde{\rho} = \rho/2M_N$  and  $\rho$  is the baryon density. The nominator  $2M_N$  arises from our choice of the Dirac spinor normalization  $\bar{u}u = 2M_N$ .  $T_{\mu\nu}^{\omega N}$  is the amplitude of the Compton  $\omega N$  scattering. For our purpose we decompose it into longitudinal and transverse parts

$$-T_{\mu\nu} = T^L P_{\mu\nu}^L + T^T P_{\mu\nu}^T \quad (16)$$

leading to  $\Pi_\omega^{L(T)} = \Pi_\omega^{\text{vac}} - \tilde{\rho} T^{L(T)}$  with  $\Pi_\omega^{\text{vac}} = g^{\mu\nu} \Pi_{\omega\mu\nu}^{\text{vac}}/3$ . The vacuum self-energy determines the properties of  $\omega$  meson in vacuum, its decay width and the mass according to

$$\begin{aligned} M_\omega \Gamma_\omega &= -\text{Im} \Pi_\omega^{\text{vac}}(q^2 = M_\omega^2) , \\ M_\omega^2 &= M_{\omega 0}^2 + \text{Re} \Pi_\omega^{\text{vac}}(q^2 = M_\omega^2) , \end{aligned} \quad (17)$$

and is discussed in many papers (cf. [15, 31]). Our choice, based on the dominance of the  $\omega \rightarrow \rho\pi$  transition (Gell-Mann, Sharp, Wagner mechanism [32]), is close to that of Ref. [15] and is described in Appendix A. The smoothly varying function  $\text{Re} \Pi_\omega^{\text{vac}}$  is absorbed in the mass parameter via  $M_{\omega 0} \rightarrow M_\omega$ .

In general, the  $\omega N$  scattering amplitude can be expressed as a sum of two tensors

$$T_{\mu\nu} = a(p, q) P_{\mu\nu}^0 + b(p, q) P_{\mu\nu}^1 , \quad (18)$$

where

$$P_{\mu\nu}^1 = g_{\mu\nu} - \frac{p_\mu q_\nu + p_\nu q_\mu}{p \cdot q} + \frac{p_\mu p_\nu q^2}{(p \cdot q)^2} , \quad (19)$$

and  $P_{\mu\nu}^0$  is defined in Eq. (4). Then, using the relations

$$\begin{aligned} P_{\mu\nu}^1 P^{T\mu\nu} &= 2, & P_{\mu\nu}^0 P^{T\mu\nu} &= 2 , \\ P_{\mu\nu}^1 P^{L\mu\nu} &= \frac{p^2 q^2}{(p \cdot q)^2}, & P_{\mu\nu}^0 P^{L\mu\nu} &= 1 , \end{aligned} \quad (20)$$

one gets

$$T^T = a(p, q) + b(p, q), \quad T^L = a(p, q) + \frac{p^2 q^2}{(p \cdot q)^2} b(p, q) . \quad (21)$$

The difference between the transversal and the longitudinal parts of the  $\omega$  meson self-energy is

$$\Pi^T - \Pi^L = \frac{1 - \gamma^2}{\gamma^2} b(p, q) = \frac{\mathbf{q}^2}{\omega^2} b(p, q) . \quad (22)$$

One can see that the absolute value of this difference increases with the  $\omega$  meson momentum and is quantified by the above defined  $\omega$  meson decay asymmetry.

In order to illustrate the effect of such a difference we utilize a resonance model for the  $\omega N$  elastic scattering, depicted schematically in Fig. 2.

The amplitude is calculated as a sum of the tree-level  $s$ -channel amplitudes shown in Fig. 2 (a), where the imaginary part is evaluated using the Cutkosky cutting rule. Thus,

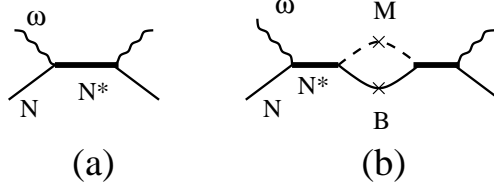


FIG. 2: (a) Tree-level diagram for the Compton  $\omega N$  scattering through nucleon resonance excitations. (b) Schematic presentation of the imaginary part of the amplitude evaluated by cutting the intermediate baryon ( $B$ ) and meson ( $M$ ) lines.

the contribution of an individual resonance to the imaginary part of  $T^{\mu\nu}$  is given as a sum of the cutted diagrams with intermediate two particle states of  $BM$  configurations shown in Fig. 2 (b) with  $B = N, \Lambda, \Delta$  and  $M = \pi, \eta, K, \sigma \rightarrow 2\pi, \rho \rightarrow 2\pi, \omega \rightarrow 3\pi$

$$\text{Im}T_r^{\mu\nu} = \sum_i \frac{p_i}{32\pi\sqrt{s}} \int \text{Tr}[T_{ri}^\mu T_{ri}^{\nu*}] d\cos\theta_i. \quad (23)$$

Here  $p_i$  and  $\theta$  are the momentum of the intermediate meson of species  $i$  and its polar angle in the  $\omega N$  center of mass system, respectively;  $s$  is the square of the total energy.  $T_{r\mu}^\alpha \lambda_\alpha$ , where  $\lambda_\alpha$  is polarization vector of the  $\omega$  meson, is the amplitude of the  $\omega N \rightarrow NM$  transition via the intermediate excitation of the resonance  $N_r^*$ .

Evaluating the real part of  $T^{\mu\nu}$  we use the following assumption

$$\text{Re}T_r^{\mu\nu} = -\text{Im}T_r^{\mu\nu} \frac{s - M_r^2}{M_r \Gamma_r}, \quad (24)$$

where  $M_r$  and  $\Gamma_r$  are the mass and the total decay width of the resonance  $r$ , respectively. The latter one depends on  $s$ . This ansatz is motivated by the standard presentation of the resonant amplitude as

$$T_r = \frac{A_r}{s - M_r^2 + iM_r\Gamma_r} \quad (25)$$

which is widely used in similar analyses, e.g. in Ref. [33, 34]. Note that, if one could calculate the resonant amplitude shown in Fig. 2 (a), using the standard Feynman rules, then Eq. (24) would be exact. Our analysis shows that for the most of important resonances the imaginary part calculated either by Eq. (23) or by a direct calculation of the diagram shown in Fig. 2 (a) are very close to each other which encourage the use of the ansatz Eq. (24). Using Eqs. (23) and (24), one can derive the amplitudes  $T^{TL}$  explicitly at finite momentum  $\mathbf{q}$  and perform a quantitative analysis of the decay asymmetry. This is the advantage of such a simplified

model. The disadvantage consists in a loss of the  $S$  matrix unitarity due to lacking coupling to additional transitions. This is a typical approximation for approaches based on tree-level diagrams. Since the aim of the present paper is to show the qualitative effect in the decay asymmetry, we leave a more detailed quantitative analysis of the Compton amplitude (based, for example, on the coupled channel approach of Ref. [15]) for future studies.

Evaluating the  $\omega NN^*$  interaction we utilize the resonance model previously used for the  $\omega$ -meson photo-production in Ref. [18] within the effective Lagrangian formalism. We consider isospin  $I = 1/2$  and spin  $J \leq 5/2$  nucleon resonances listed in [35] with the empirically known helicity amplitudes of  $\gamma N \rightarrow N^*$  transitions, because the  $\omega NN^*$  coupling constants are defined within the vector dominance model. Exceptions are the  $P_{11}(1710)$  and  $D_{13}(2080)$  resonances for which one can evaluate the  $\omega NN^*$  coupling constants from known partial decay widths for  $N^* \rightarrow \omega N$  [14, 35]. We thus start our analysis by taking into account contributions of the following 10 resonances:  $P_{11}(1440)$ ,  $D_{13}(1520)$ ,  $S_{11}(1535)$ ,  $S_{11}(1650)$ ,  $D_{15}(1675)$ ,  $F_{15}(1680)$ ,  $D_{13}(1700)$ ,  $P_{11}(1710)$ ,  $P_{13}(1720)$ , and  $D_{13}(2080)$ . However, it turns out that only six of them give a sizable contribution. These are  $D_{13}(1520)$ ,  $S_{11}(1535)$ ,  $F_{15}(1680)$ ,  $D_{13}(1700)$ ,  $P_{11}(1710)$ , and  $D_{13}(2080)$ .

For the  $N^*$  resonances with spin  $J = 1/2$ , the effective Lagrangians for the  $\omega NN^*$  interactions are chosen to be of the form of tensor coupling. This "minimal" form of Lagrangians, previously used in the study of  $\eta$  photo-production [36], is

$$\mathcal{L}_{\omega NN^*}^{\frac{1}{2}^{\pm}} = \frac{g_{\omega NN^*}}{2M_{N^*}} \bar{\psi}_{N^*} \Gamma^{(\pm)} \sigma_{\mu\nu} F^{\mu\nu} \psi_N + \text{h.c.}, \quad (26)$$

where  $\psi_N$  and  $\psi_{N^*}$  are the nucleon, and nucleon resonance fields, respectively, and  $F^{\mu\nu} = \partial^\nu \omega^\mu - \partial^\mu \omega^\nu$ , and  $\omega_\mu$  is the  $\omega$  meson field. The coupling  $\Gamma^+ = 1$  ( $\Gamma^- = \gamma_5$ ) defines the excitation of a positive (negative) parity  $N^*$  state.

For the  $N^*$  resonances with spin  $J = 3/2$ , we use the expression introduced in Refs. [36–38]

$$\mathcal{L}_{\omega NN^*}^{\frac{3}{2}^{\pm}} = i \frac{g_{\omega NN^*}}{M_{N^*}} \bar{\psi}_{N^*}^\mu O_{\mu\nu}(Z) \gamma_\lambda \Gamma^{(\mp)} F^{\lambda\nu} \psi_N + \text{h.c.}, \quad (27)$$

where  $\psi_\alpha$  is the Rarita-Schwinger baryon field. The off-shell operator  $O_{\mu\nu}(Z)$  is

$$O_{\mu\nu}(Z) = g_{\mu\nu} - \left[ \frac{1}{2} + Z \right] \gamma_\mu \gamma_\nu, \quad (28)$$

where  $Z$  is the so-called "off-shell" parameter.

The effective Lagrangians for the resonances with  $J^P = \frac{5}{2}^\pm$  are constructed by analogy with the previous case,

$$\mathcal{L}_{\omega NN^*}^{\frac{5}{2}^\pm} = \frac{g_{\omega NN^*}}{M_{N^*}^2} \bar{\psi}_{N^*}^{\mu\alpha} O_{\mu\nu}(Z) \gamma_\lambda \Gamma^{(\pm)} (\partial_\alpha F^{\lambda\nu}) \psi_N + \text{h.c.}, \quad (29)$$

where  $\psi_{\alpha\beta}$  is the spin-5/2 field.

The  $\omega NN^*$  coupling is defined by using the vector dominance model, which gives a relation between  $g_{\omega NN^*}$  and the iso-scalar electromagnetic coupling  $eg_{\gamma NN^*}^s$ . The determination of  $eg_{\gamma NN^*}^s$  is described in Ref. [18]. For the sake of convenience, we list the employed coupling constants  $g_{\omega NN^*}$  in Appendix B. There we also list the effective Lagrangians of the  $N^* BM$  interaction and the corresponding strength parameters. Following [18] we choose the off-shell parameter  $Z = -1/2$  for all  $N^*$ . Calculating the amplitude of the  $\omega N \rightarrow N^* \rightarrow BM$  process we parameterize the off-shell form factor of  $N^*$  by the covariant function

$$F_{N^*}(p^2) = \frac{\Lambda_{N^*}^4}{\Lambda_{N^*}^4 + (p^2 - M_{N^*}^2)^2}. \quad (30)$$

The cut-off parameter  $\Lambda_N = 0.85$  GeV is taken to be the same for all resonances. The invariant amplitude of the transition  $\omega N \rightarrow N^* \rightarrow Ni$  has the form of Eq. (25), where the energy dependent total decay width is calculated according to Ref. [39],

$$\Gamma^{\text{tot}}(W) = \sum_j \Gamma_j \frac{\rho(W)}{\rho(M_{N^*})}, \quad (31)$$

where  $\Gamma_j$  is the partial width for the resonance decay into channel  $j$ , evaluated at  $W = \sqrt{s} = M_{N^*}$ . The form of the "phase space-factor"  $\rho(W)$  depends on the decay channel, the relative momenta  $k_j$  of the outgoing particles, and their relative orbital momenta  $l_j$ . It provides the proper analytic threshold behavior  $\rho(W) \sim k_j^{2l_j+1}$  and becomes constant at high energy [40].

In case of  $J = 3/2$  resonances we use the covariant modification of the Rarita-Schinger propagator  $\mathcal{P}_{\alpha\beta}$ , as suggested by Pascalutsa in [41]. For  $J = 5/2$  resonances, we use the covariant propagator  $\mathcal{P}_{\alpha\beta,\delta\gamma}$  introduced in Ref. [42].

#### IV. RESULTS AND DISCUSSION

First of all let us note that the  $\omega N \rightarrow F_{15}$  transition comes through the orbital interaction with  $L = 1, 3$  and, therefore, the resonance  $F_{15}$  does not contribute to the  $\omega$  meson self-energy at  $|\mathbf{q}| = 0$ . Formally, it follows from the identity  $\mathcal{P}_{\alpha\beta,\gamma\delta} q^\alpha = 0$ , at  $\mathbf{q} = 0$ . Thus, at

$|\mathbf{q}| = 0$  the main contribution stems from the excitation of the  $D_{13}$  resonances. However, when  $|\mathbf{q}|$  increases, the contribution of the  $F_{15}$  resonance becomes important.

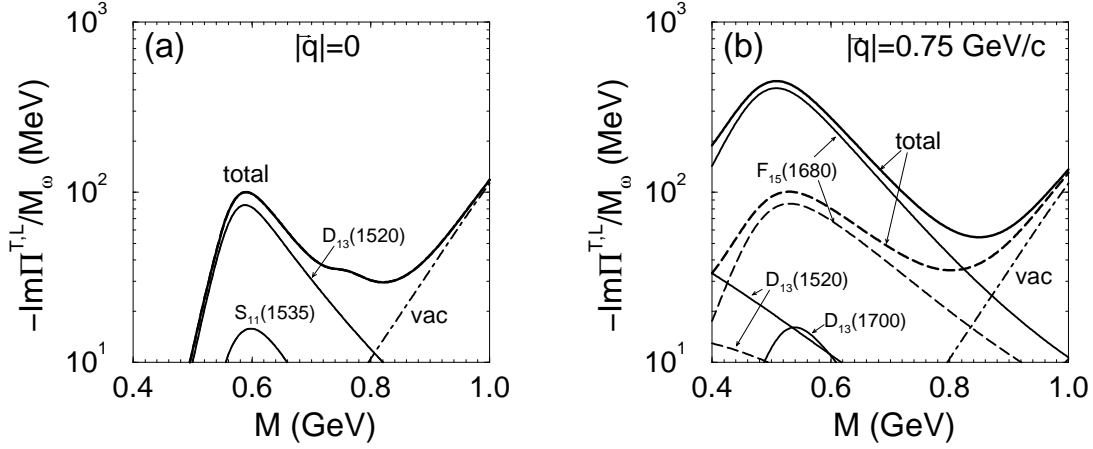


FIG. 3: The imaginary part of the  $\omega$  meson self-energy at  $\mathbf{q} = 0$  (a) and  $0.75 \text{ GeV}/c$  (b). The thin solid and dashed curves in (b) correspond to the transverse and longitudinal components, respectively. The thick solid curves correspond to the total contributions. The vacuum contribution is depicted by dot-dashed curves.

The imaginary part of the  $\omega$  meson self-energy is presented in Fig. 3. We show the ratio  $-\text{Im}\Pi^{TL}/M_\omega$  which approximately corresponds to the modified  $\omega$  meson decay width. The case of  $|\mathbf{q}| = 0$  is shown in Fig. 3 (a). One can see that the main contribution in our model comes, indeed, from the  $D_{13}(1520)$  excitation. The next important resonance is  $S_{11}(1535)$ . The contribution of other resonances is negligible. For  $|\mathbf{q}| = 0.75 \text{ GeV}/c$  the situation changes. The dominant contribution comes now from the  $F_{15}$  resonance, while the  $D_{13}$  excitations are much weaker. One can see a sizable difference between transverse and longitudinal parts of the self-energy.

The real part of the self-energy is presented in Fig. 4. Here we show the ratio  $\text{Re}\Pi^{TL}/(M + M_\omega)$  which corresponds to the shift of the pole position of the  $\omega$  meson propagator in medium. Similar to the previous case, for  $|\mathbf{q}| = 0$  the main contribution comes from the  $D_{13}(1520)$  excitation, while at  $|\mathbf{q}| = 0.75 \text{ GeV}/c$  the  $F_{15}$  resonance is dominant.

The quantities  $W^{T,L}$  as a function of the  $\omega$  meson mass  $M$  are presented in Fig. 5. The vacuum case is shown by the dot-dashed curve. It is evident that the model predicts some (upward) shift of the pole position which increases from  $\Delta M = 8$  to 20 (40) MeV for the longitudinal (transverse) part when  $|\mathbf{q}|$  changes from 0 to  $0.75 \text{ GeV}/c$ .

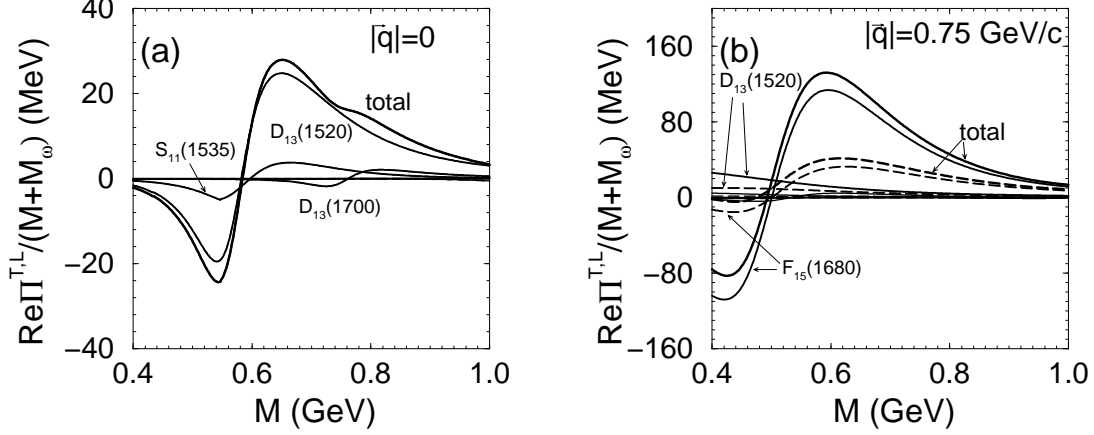


FIG. 4: The real part of the  $\omega$  meson self-energy. Notation as in Fig. 3

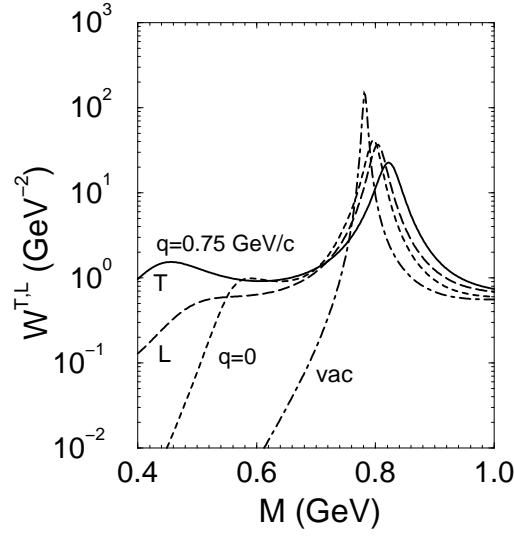


FIG. 5: The functions  $W^{T,L}$  for different values  $|\mathbf{q}|$ . The solid (dashed) curve depicts  $W^T$  ( $W^L$ ). The vacuum case is shown by dot-dashed curve.

Our result for the decay asymmetry is exhibited in Fig. 6. We display the asymmetry  $\mathcal{A}^{TL}$  as a function of the  $\omega$  meson mass for different values of  $|\mathbf{q}|$ . The asymmetry is zero at  $|\mathbf{q}| = 0$ . At finite  $|\mathbf{q}|$  and  $M \sim M_\omega$ , it becomes a non-trivial function of  $M$  and it is defined by the interplay of the different resonances, as seen in the left panel of Fig. 6. One can see that the sign and the amplitude of the asymmetry depends strongly on both  $|\mathbf{q}|$  and  $M$  and is sensitive to the details of the resonance model. For  $|\mathbf{q}| \simeq 0.75$  GeV/c the asymmetry is mainly determined by the contribution of the  $F_{15}$  resonance. At  $M \leq 0.7$  it is positive and monotonically increases with decreasing  $M$ . At  $M \sim M_\omega$  (see Fig. 6 (b)) its non-monotonic behavior is determined by the difference of the peak positions for  $W^T$  and  $W^L$ . The shape

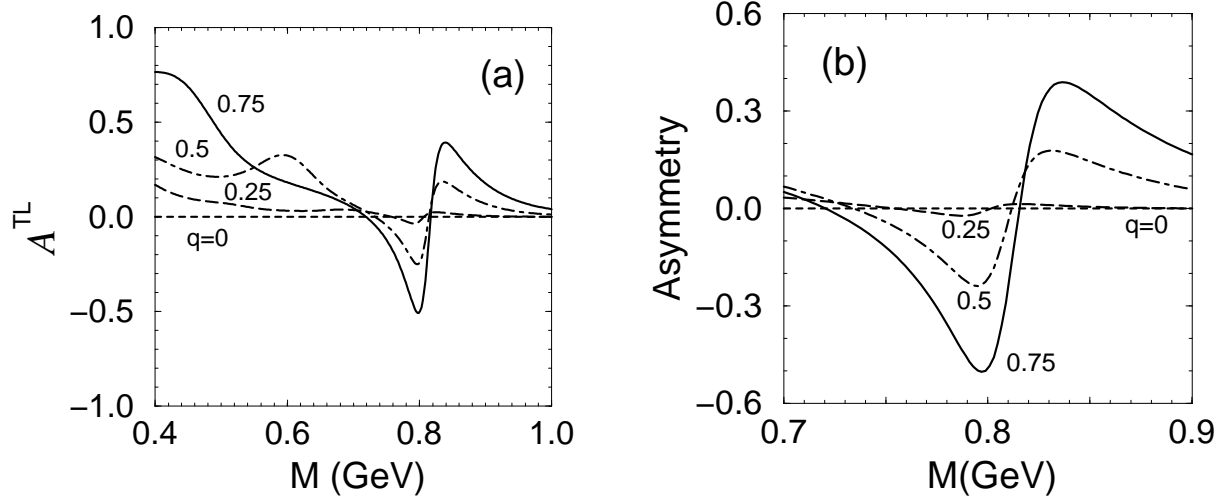


FIG. 6: (a) The  $\omega$  meson decay asymmetry for different values  $|q|$ . (b) The same as in (a) but at  $M \sim M_\omega$ .

of this curve again is sensitive to the details of the resonance model.

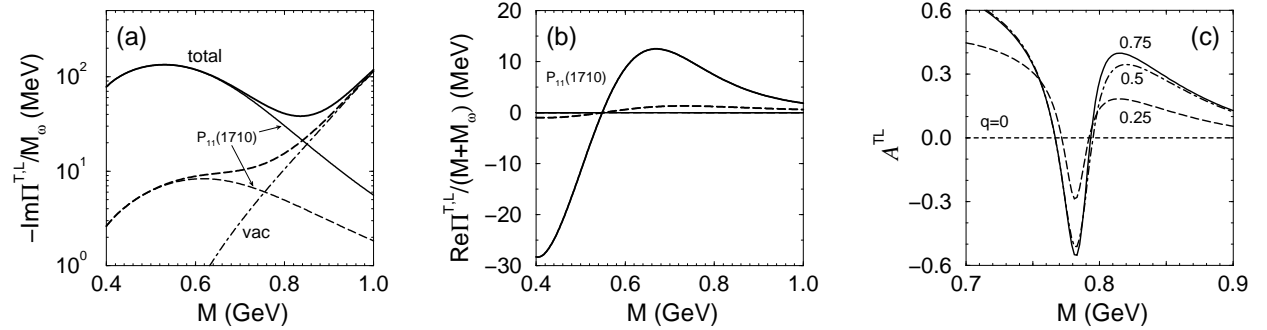


FIG. 7: Results for the resonance model dominated by the  $P_{11}(1710)$  resonance. (a) and (b) are for the imaginary and real parts of the  $\omega$  meson self-energy, respectively, while (c) exhibits the decay asymmetry.

Note that our result for  $\Pi_\omega^{T,L}$  in medium is qualitatively similar to that of Ref. [15] obtained within a coupled channel approach. Therefore, we expect that the asymmetry for the model [15] would be also close to our result.

In order to demonstrate the sensitivity of the asymmetry to the actually employed resonance model we show in Fig. 7 results for the resonance model developed in Ref. [24] for the reaction  $pp \rightarrow \omega pp$ . Here, the dominant contribution comes from the  $P_{11}(1710)$  resonance with the  $\omega NN^*$  coupling constant, rewritten in our notation,  $g_{\omega NN^*} = 10.32$ , i.e. 4.9 times larger than ours. The dependence of the polarization operators on the momentum  $\mathbf{q}$

is different, and this difference is manifest in the asymmetry. Thus, there is no dramatic change of the asymmetry if  $|\mathbf{q}|$  increases from 0.25 to 0.75 GeV/c, as seen in Fig. 7. To illustrate the difference between the two models, we exhibit in Fig. 8 simultaneously the asymmetry for these two models: the resonance model developed in Sec. III (curves labelled by A) and the model [24], dominated by the  $P_{11}(1710)$  resonance (curves labelled by B). One can see a strong difference in the dependence on  $M$  at fixed  $|\mathbf{q}| = 0.75$  GeV/c. Also the dependence on  $|\mathbf{q}|$  at fixed  $M = 0.7$  GeV is rather different. Such a difference in the  $M$  vs.  $|\mathbf{q}|$  dependence may be used as a tool for studying the nature of the  $\omega$  meson self-energy.

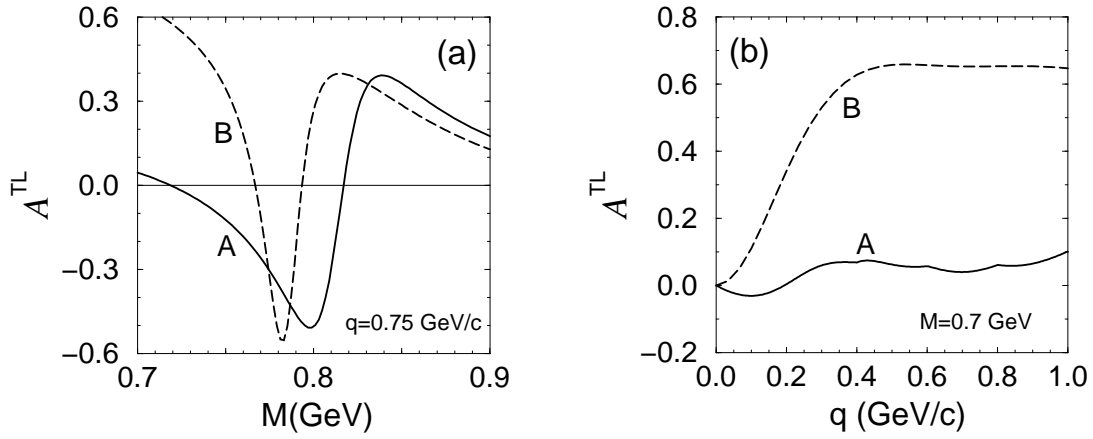


FIG. 8: The  $\omega$  meson decay asymmetry for models A and B depicted by solid and dashed curves. (a) dependence on  $M$  at  $|\mathbf{q}| = 0.75$  GeV/c, (b) dependence on  $|\mathbf{q}|$  at  $M = 0.7$  GeV.

## V. SUMMARY

In summary we discuss an asymmetry of the  $\omega \rightarrow e^+e^-$  decay with respect to the electron and positron energies in the nuclear-matter rest-system. Thereby, we suppose that the  $\omega$  meson is created by an elementary projectile impinging on a heavy target nucleus. The asymmetry is zero for the  $\omega$  meson at rest and it is non-zero at non-zero  $\omega$  momentum. We find that the asymmetry is sensitive to the properties of the  $\omega$  meson self-energy and, in particular, it has a non-trivial dependence on the  $\omega$  mass (energy) and momentum. We have shown that the excitation of high-spin resonances results in a strong momentum dependence of the asymmetry around  $M = 0.75 - 0.8$  GeV and it is flat at  $M = 0.7$  GeV. Therefore, the asymmetry may be used as a powerful tool in studying the properties of the  $\omega$  meson in a nuclear medium. Our analysis is performed by using a simple resonance model where

the coupling between  $\omega N$  and  $MB$  ( $M = \pi, \eta, \sigma, \rho, K$ ;  $B = N, \Delta, \Lambda$ ) channels is taking into account only in evaluating the imaginary part of the Compton  $\omega N$  elastic scattering amplitude. An interesting subject for further investigations is to study this asymmetry within more sophisticated models, say within a consistent description of coupled channels as well as on the basis of the QCD inspired models. Experimentally, the asymmetry can be studied at various facilities, e.g., KEK, HADES at GSI etc.

## Acknowledgments

We would like to thank V. Shklyar for fruitful discussions. One of the authors (A.I.T.) appreciates the FZD for the hospitality. This work was supported by BMBF grant 06DR136 and GSI-FE.

## APPENDIX A: $\omega$ MESON SELF-ENERGY IN VACUUM

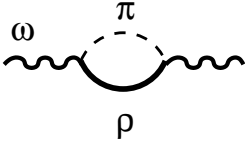


FIG. 9: The  $\omega$  meson self-energy in vacuum.

We assume the dominance of the virtual  $\omega \rightarrow \rho\pi$  vacuum transitions, depicted in Fig. 9. This transition is described by the effective Lagrangian in obvious standard notations

$$\mathcal{L} = \frac{g_{\omega\rho\pi}}{M_\omega} \epsilon^{\mu\nu\alpha\beta} \partial_\mu \omega_\alpha \partial_\nu \rho_\beta . \quad (\text{A1})$$

The imaginary part of  $\Pi^{\text{vac}}$  is calculated, using Cutkosky rules, as

$$\text{Im } \Pi_\omega^{\text{vac}}(q^2) = -\frac{g_{\omega\rho\pi}^2 \sqrt{q^2}}{12\pi M_\omega^2} p^3(q^2, M_\rho^2) , \quad (\text{A2})$$

with  $p^2(q^2, M_\rho^2) = \lambda(q^2, M_\rho^2, M_\pi^2)/(4q^2)$ . Taking into account the  $\rho$  meson mass distribution in the region  $2M_\pi < M_\rho < \sqrt{q^2} - M_\pi$  and normalizing  $\text{Im } \Pi_\omega^{\text{vac}}(M_\omega^2)$  to the total decay width  $\Gamma_\omega$  we get

$$\text{Im } \Pi_\omega^{\text{vac}}(q^2) = -\sqrt{q^2} \Gamma_\omega \frac{G(\sqrt{q^2})}{G(M_\omega)} \quad (\text{A3})$$

with

$$G(x) = \int_{2M_\pi}^{x-M_\pi} \frac{p^3(x^2, y^2) y dy}{(y^2 - M_\rho^2)^2 + (M_\rho \Gamma_\rho)^2} , \quad (\text{A4})$$

where  $\Gamma_\rho = 149.2$  MeV is the total  $\rho$  meson decay width.

The real part of the self-energy depends on the regularization scheme. Its absolute value is comparable, in order of magnitude, with the absolute value of the imaginary part being much smaller than the square of the physical  $\omega$  meson mass. Therefore, to avoid unknown parameters, we simply put the combination  $M_{\omega 0}^2 + \text{Im} \Pi_\omega^{vac}(q^2) \simeq M_{\omega 0}^2 + \text{Im} \Pi_\omega^{vac}(M_\omega^2)$  in denominator of Eq. (16) to be equal  $M_\omega^2$ , with replacing  $M_{\omega 0}^4 \rightarrow M_\omega^4$  in the numerator.

## APPENDIX B: FIXING PARAMETERS OF THE RESONANCE MODEL

### 1. Effective Lagrangians for the $N^* \rightarrow \mu B$ transitions

Consider first the virtual  $N^* \rightarrow \mu N$  transitions with  $\mu = \pi, \eta, \sigma, \rho, \omega$ . The effective Lagrangian for the  $\rho NN^*$  interaction is taken to be the same as for  $\omega NN^*$  (cf. Eqs. (26) - (29)) with obvious generalization for the isospin  $I_\rho = 1$ ). The interactions written in standard notation read

$$\mathcal{L}_{\mu NN^*}^{\frac{1}{2}\pm} = \bar{\psi}_{N^*} \left[ g_{\pi NN^*} \Gamma^\mp \boldsymbol{\pi} \cdot \boldsymbol{\tau} + g_{\eta NN^*} \Gamma^\mp \eta + g_{\sigma NN^*} \Gamma^\pm \sigma \right] \psi_N + \text{h.c.} , \quad (\text{B1})$$

$$\mathcal{L}_{\mu NN^*}^{\frac{3}{2}\pm} = \bar{\psi}_{N^*}^\alpha \left[ \frac{g_{\pi NN^*}}{M_{N^+}} \Gamma^\pm \partial_\alpha \boldsymbol{\pi} \cdot \boldsymbol{\tau} + \frac{g_{\eta NN^*}}{M_{N^+}} \Gamma^\pm \partial_\alpha \eta + \frac{g_{\sigma NN^*}}{M_{N^+}} \Gamma^\mp \partial_\alpha \sigma \right] \psi_N + \text{h.c.} , \quad (\text{B2})$$

$$\mathcal{L}_{\mu NN^*}^{\frac{5}{2}\pm} = i \bar{\psi}_{N^*}^{\alpha\beta} \left[ \frac{g_{\pi NN^*}}{M_{N^+}} \Gamma^\mp \partial_\alpha \partial_\beta \boldsymbol{\pi} \cdot \boldsymbol{\tau} + \frac{g_{\eta NN^*}}{M_{N^+}} \Gamma^\mp \partial_\alpha \partial_\beta \eta + \frac{g_{\sigma NN^*}}{M_{N^+}} \Gamma^\pm \partial_\alpha \partial_\beta \sigma \right] \psi_N + \text{h.c.} , \quad (\text{B3})$$

where  $\Gamma^+ = 1$  and  $\Gamma^- = \gamma_5$ . The interactions  $N^* \rightarrow K \Lambda$  are similar to  $N^* \rightarrow \eta N \Lambda$  with substitutions  $\eta \rightarrow K$  and  $N \rightarrow \Lambda$ . The interactions  $N^* \rightarrow \pi \Delta$  are chosen as

$$\mathcal{L}_{\pi \Delta N^*}^{\frac{1}{2}\pm} = i \frac{g_{\pi \Delta N^*}}{N^*} \bar{\psi}_{N^*} \Gamma^\pm \partial_\alpha K \psi_\Delta^\alpha + \text{h.c.} , \quad (\text{B4})$$

$$\mathcal{L}_{\pi \Delta N^*}^{\frac{3}{2}\pm} = g_{\pi \Delta N^*} \bar{\psi}_{N^*}^\alpha \Gamma^\mp \psi_{\Delta\alpha} K + \text{h.c.} , \quad (\text{B5})$$

$$\mathcal{L}_{\pi \Delta N^*}^{\frac{5}{2}\pm} = i \frac{g_{\pi \Delta N^*}}{N^*} \bar{\psi}_{N^*}^{\alpha\beta} \Gamma^\pm \partial_\beta K \psi_{\Delta\alpha} + \text{h.c.} . \quad (\text{B6})$$

## 2. $N^*BM$ coupling constants

In Table I we present the coupling constants of  $N^* \rightarrow BM$  transitions for the dominant amplitudes.

TABLE I: The coupling constants of the employed effective Lagrangians. The  $g_{\omega NN^*}$  coupling constants are from Ref. [18] (Model II) using the vector dominance model. For  $P_{11}(1710)$  and  $D_{13}(2080)$  it is deduced from the branching ratios of  $N^* \rightarrow N\omega$  decays being 13% and 21% [35]. Other coupling constants are found by fitting the corresponding branching ratios of the  $N^* \rightarrow N\mu$  decay taken from Ref. [35] and shown in parentheses (in %). We show only absolute values of the coupling constant, as their phases drop out in our calculations.

$N^*$	$M_{N^*}$	$g_{\omega NN^*}$	$g_{\pi NN^*}$	$g_{\eta NN^*}$	$g_{\sigma NN^*}$	$g_{\rho NN^*}$	$g_{K\Lambda N^*}$	$g_{\pi\Delta N^*}$
$S_{11}$	1535	2.14	0.684(45)	2.12(55)	—	—	—	—
$P_{11}$	1710	2.12(13)	2.28(15)	4.22(6.2)	1.51(25)	1.13(15)	13.4(15)	1.66(10.8)
$D_{13}$	1520	5.70	17.9(60)	—	—	1.40(20)	—	0.365(20)
$D_{13}$	1700	1.16	5.36(15)	—	6.77(82)	—	4.97(3)	—
$D_{13}$	2080	2.91(21)	8.27(23)	11.0(7)	—	—	—	0.708(49)
$F_{15}$	1680	35.0	62.0(65)	—	21.1(25)	—	—	1.72(10)

- 
- [1] R. Rapp and J. Wambach, Adv. Nucl. Phys. **25**, 1 (2000).
  - [2] D. Trnka *et al.* [CBELSA/TAPS Collaboration], Phys. Rev. Lett. **94**, 192303 (2005) [arXiv:nucl-ex/0504010].
  - [3] M. Naruki *et al.*, Phys. Rev. Lett. **96**, 092301 (2006) [arXiv:nucl-ex/0504016].
  - [4] J. C. Caillon and J. Labarsouque, J. Phys. G **21**, 905 (1995).
  - [5] F. Klingl, N. Kaiser and W. Weise, Nucl. Phys. A **624**, 527 (1997).
  - [6] F. Klingl, T. Waas and W. Weise, Nucl. Phys. A **650**, 299 (1999).
  - [7] K. Saito, K. Tsushima, A. W. Thomas and A. G. Williams, Phys. Lett. B **433**, 243 (1998).
  - [8] A. K. Dutt-Mazumder, Nucl. Phys. A **713**, 119 (2003).
  - [9] S. Zschocke, O. P. Pavlenko and B. Kämpfer, Phys. Lett. B **562**, 57 (2003).
  - [10] M. Post and U. Mosel, Nucl. Phys. A **688**, 808 (2001).

- [11] M. F. M. Lutz, G. Wolf and B. Friman, Nucl. Phys. A **706**, 431 (2002), erratum-ibid. A **765**, 431 (2006).
- [12] A. K. Dutt-Mazumder, R. Hofmann and M. Pospelov, Phys. Rev. C **63**, 015204 (2001).
- [13] B. Steinmueller and S. Leupold, Nucl. Phys. A **778**, 195 (2006).
- [14] G. Penner and U. Mosel, Phys. Rev. C **66**, 055211 (2002).
- [15] P. Mühlich, V. Shklyar, S. Leupold, U. Mosel and M. Post, Nucl. Phys. A **780**, 187 (2006).
- [16] C. B. Dover, J. Hüfner and R. H. Lemmer, Annals Phys. **66**, 248 (1971).
- [17] J. Ajaka *et al.*, Phys. Rev. Lett. **96**, 132003 (2006).
- [18] A. I. Titov and T. S. H. Lee, Phys. Rev. C **66**, 015204 (2002).
- [19] G. Penner and U. Mosel, Phys. Rev. C **66**, 055212 (2002).
- [20] V. Shklyar, H. Lenske, U. Mosel, and G. Penner, Phys. Rev. C **71**, 055206 (2005).
- [21] Q. Zhao, Phys. Rev. C **63**, 025203 (2001).
- [22] G. Penner and U. Mosel, Phys. Rev. C **66**, 055211 (2002).
- [23] M. F. M. Lutz, G. Wolf and B. Friman, Heavy Ion Phys. **17**, 313 (2003); Prog. Theor. Phys. Suppl. **149**, 152 (2003).
- [24] K. Tsushima and K. Nakayama, Phys. Rev. C **68**, 034612 (2003).
- [25] C. Fuchs, M. I. Krivoruchenko, H. L. Yadav, A. Faessler, B. V. Martemyanov and K. Shekhter, Phys. Rev. C **67**, 025202 (2003).
- [26] H. A. Weldon, Phys. Rev. D **42**, 2384 (1990).
- [27] C. Gale and J. I. Kapusta, Nucl. Phys. B **357**, 65 (1991).
- [28] A. I. Titov, T. I. Gulamov and B. Kämpfer, Phys. Rev. D **53**, 3770 (1996).
- [29] T. I. Gulamov, A. I. Titov and B. Kämpfer, Phys. Lett. B **372**, 187 (1996).
- [30] N. M. Kroll, T. D. Lee and B. Zumino, Phys. Rev. **157**, 1376 (1967).
- [31] F. Klingl, N. Kaiser and W. Weise, Z. Phys. A **356**, 193 (1996).
- [32] M. Gell-Mann, D. Sharp and W. G. Wagner, Phys. Rev. Lett. **8**, 261 (1962).
- [33] V. L. Eletsky, M. Belkacem, P. J. Ellis and J. I. Kapusta, Phys. Rev. C **64**, 035202 (2001).
- [34] A. T. Martell and P. J. Ellis, Phys. Rev. C **69**, 065206 (2004).
- [35] W. M. Yao *et al.* [Particle Data Group], J. Phys. G **33**, 1 (2006).
- [36] M. Benmerrouche, N.C. Mukhopaghyay, and J.F. Zhang, Phys. Rev. D **51**, 3237 (1995).
- [37] R.M. Davidson, N.C. Mukhopaghyay, and R.S. Wittman, Phys. Rev. D **43**, 71 (1991).
- [38] M.G. Olsson and E.T. Osipovsky, Nucl. Phys. **B 87**, 399 (1975).

- [39] D. M. Manley and E. M. Saleski, Phys. Rev. D **45**, 4002 (1992).
- [40] D. M. Manley, R. A. Arndt, Y. Goradia and V. L. Teplitz, Phys. Rev. D **30**, 904 (1984).
- [41] V. Pascalutsa, Phys. Rev. D **58**, 096002 (1998).
- [42] V. Shklyar, G. Penner and U. Mosel, Eur. Phys. J. A **21**, 445 (2004).